RM-613

M551 METALS MELTING EXPERIMENT

February 1976

(NASA-CR-149927) M551 METALS MELTING EXPERIMENT (Grumman Aerospace Corp.) 26 p
CSCL 11F
N76-27401
Unclas
G3/26 44797

RESEARCH DEPARTMENT

GRUMMAN AEROSPACE CORPORATION
BETHPAGE NEW YORK

Grumman Research Department Memorandum RM- 613

M551 METALS MELTING EXPERIMENT+

by

C. H. Li, G. Busch, and C. Creter

Materials and Structural Mechanics

February 1976

+Prepared in partial fulfillment of Contract NAS8-28728 for NASA

Approved by:

Charles E. Mack, Jr.
Charles E. Mack, Jr.
Director of Research

TABLE OF CONTENTS

Section	Page
Introduction	1
Experimental Procedures	2
Microstructure	4
2219-T87 Aluminum	4
304L Stainless Steel	7
Tantalum	8
Copper Segregation	12
Microhardness	16
Summary.	20
References	21

LIST OF ILLUSTRATIONS

Figure		Page
1	Comparison of Skylab (top) and Ground Base (bottom) Weld Samples	5
2	Fusion Zone Microstructures in 2219-T87 Aluminum Ground Base Sample No. 3, 500X	6
3	Interfacial Microstructures in 304L Stainless Steel Sample No. 7, 500X	9
4	Copper Segregation in Eutectic Particles of 2219-T87 Aluminum Skylab Sample No. 3 in Heat Affected Zone, 1350X	13
5	Fraction of Eutectic Along Centerline of Weld in 2219-T87 Aluminum Samples No. 1	14
6	Microhardness on Cross-Section Ground Base Vs. Skylab, Sample No. 9	17

TABLES

Table		Page
1	Cu w/o in Al Sample No. 1	15
2	Summary of Microhardness on Sample No. 9	18

ABSTRACT

Results gathered to date further support our belief that the major difference between ground base and Skylab samples (i.e., large elongated grains in ground base samples versus nearly equiaxed and equal sized grains in Skylab samples) can be explained on the basis of constitutional supercooling, and not on the basis of surface phenomena.

We obtained new microstructural observations on the weld samples and present explanations for some of these observations. In particular, we studied ripples and examined their implications to weld solidification.

We also provide evidence of pronounced copper segregation in the Skylab 2219-T87 Al weld samples, and show that in the tantalum samples studied, the Skylab weld microhardness (and hence strength) is uniformly higher than the ground base results. This also is in agreement with our previous predictions.

INTRODUCTION

The M551 (Metals Melting) Skylab Experiment consisted of selectively melting, in sequence, three rotating discs made of 2219-T87 aluminum, 304L stainless steel and tantalum. For comparison, three other discs of the same three materials were similarly melted or "welded" on the ground (Refs. 1-3).

The power source of the melting was an electron beam unit operated at 20 kV and 50 to 80 mA. The electron beam (0.15 cm diameter) was kept stationary normal to the disc and at 6 cm from the axis of the disc. The discs were rotated to generate a tangential velocity relative to the normally impinging beam of 1.61 cm/sec together with a radial acceleration of 5.09×10^{-4}g (Ref. 3).

EXPERIMENTAL PROCEDURES

Representative samples of each weld material generated in the experiment were received from NASA Marshall Space Flight Center in standard metallurgical mounts. The 2219-T87 aluminum alloy and the 304L stainless steel were repolished with different grades of alumina. The tantalum alloy sections were rough polished with diamond and final polished with alumina.

The hardness surveys were conducted with a Reichert microhardness tester, which was calibrated in the following manner. First, the length constant for the optical system was calculated. The value obtained (0.05 mm $\Rrightarrow$ 0.168µm) is correct for the optics used. After zeroing the weight scale, the deflection scale was calibrated using a known series of weights from 5 to 100 grams. A plot of the scale deflection vs. applied weight agreed very well with the factory calibration curve. Hardness traverses on the samples were then made using either 50 or 100 gram loads applied for 30 seconds. Two traverses were usually made on both the cross section and the crown section. Hardness measurements were made 0.24 mm apart, except at the weld interfaces where they were made 0.1 mm apart.

The base diagonals of the diamond indentation were measured and converted to micrometers. From these values, the microhardness (H_m) was determined according to the following formula

$$H_m = 1834.4 \frac{P}{d^2} \text{ Kg/mm}^2$$

where P is the load in grams and d is the diagonal length in mm.

At the conclusion of the hardness surveys the samples were etched for further microstructural studies. The following etchants were used:

Alloy	Etchant	Features Revealed
2219-T87 Al	10ml H_3PO_4, 90ml H_2O (50°C)	Eutectic and rosette structure
	Keller's etch	General grain size and shape
304L SS	40ml HNO_3, 10ml HCl, 40ml Methanol	Sigma, and carbide phases, dendritic structure, grain size and shape
Ta - 0.5 $^w/_o$ Cb	30ml HF, 15ml HNO_3, 30ml HCl	Grain size and shape

The resulting microstructures were examined with the light microscope and selected areas of each sample were photographed at various magnifications.

Ground base and Skylab samples of aluminum (No. 3) and stainless steel (No. 7) were examined and compared in the scanning electron microscope. To enhance the images, the samples were coated with 250 Å of carbon and gold. The weld, weld interface, and heat affected zone were thoroughly examined. A cursory chemical analysis with an energy dispersive analyzer system was conducted on some of these samples.

Based on the results of the energy dispersive analysis, we decided to conduct an in-depth analysis on the aluminum alloy with the electron probe microanalyzer.

MICROSTRUCTURE

Typical microstructures of ground base and Skylab welds in the three materials are reproduced as Fig. 1. The important features are summarized below.

A. 2219-T87 Aluminum

Features

1. Longer grains occur in the ground base sample than Skylab sample, maximum 0.32 mm vs. 0.20 mm.
2. Wider grains appear in the ground base sample than Skylab sample, maximum of 0.06 mm vs. 0.04 mm.
3. In the ground base samples, the eutectic extends extensively into the heat-affected zone of the root region with some extending near the crown. In the Skylab samples, only some eutectic particles occur at the root and crown regions.
4. In the ground base samples, the dendrites are much larger at the root region than at the crown region. In the Skylab samples, the difference in size is much smaller (Fig. 2).
5. The fine-grained, first solidification layer is thicker in the ground base sample than in the Skylab sample, 50 microns vs. 25 microns.
6. The fine-grained, first solidification layer disrupts the epitaxial relation between the fusion zone and nonfusion materials.
7. The base metal in the nonfusion zones was not appreciably affected, as judged from the grain size, grain shape, aspect ratio, and etching characteristics. This is true for both the ground base and Skylab samples.

Skylab

Ground Base

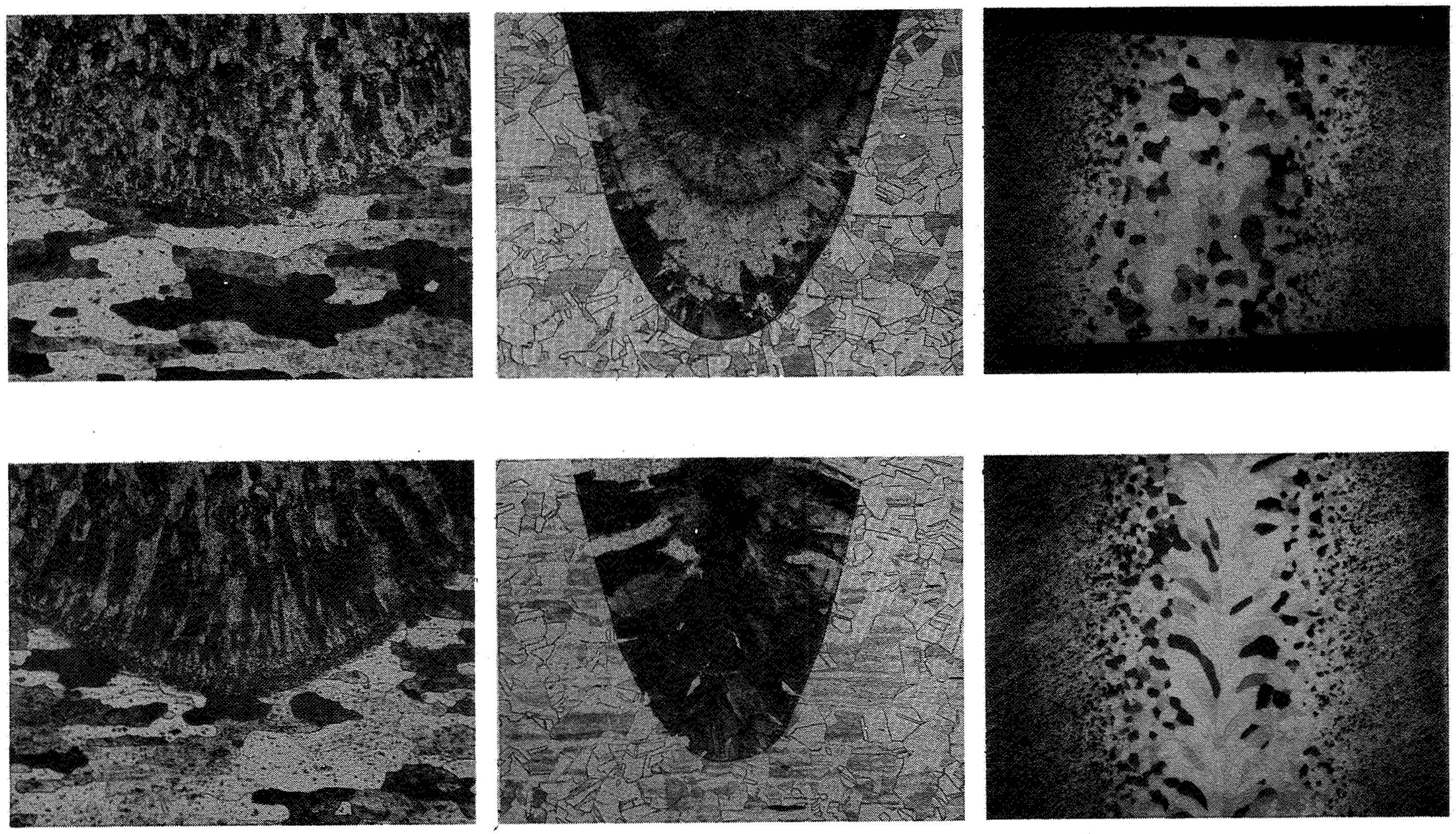

2219-T87 Aluminum, 100X | 304L Stainless Steel, 100X | Tantalum, 10X

Fig. 1 Comparison of Skylab (top) and Ground Base (bottom) Weld Samples

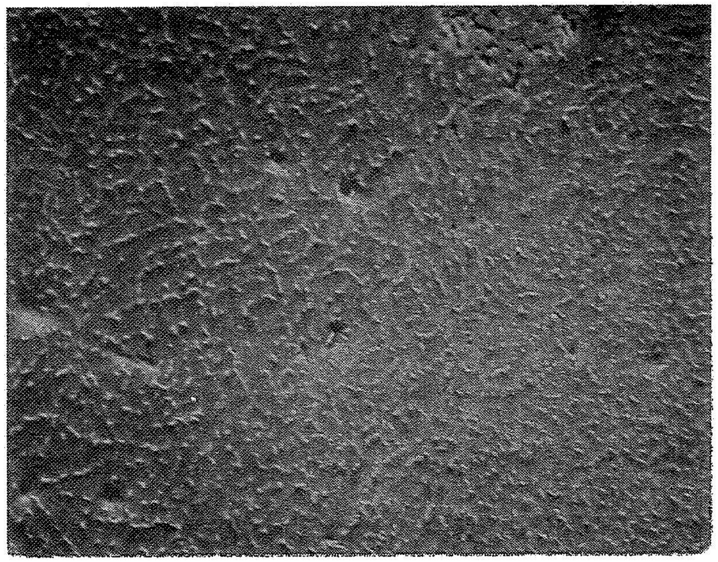

Crown Region, Small Dendrites

Root Region, Large Dendrites

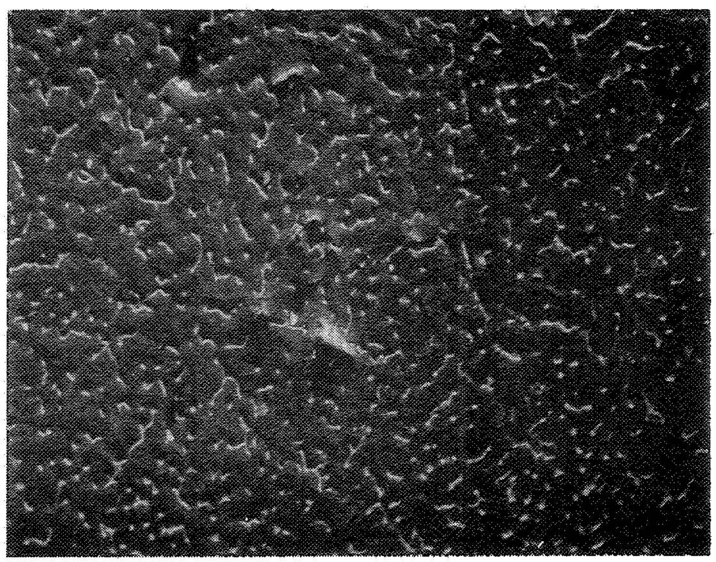

Crown Region, Dendritic Structure

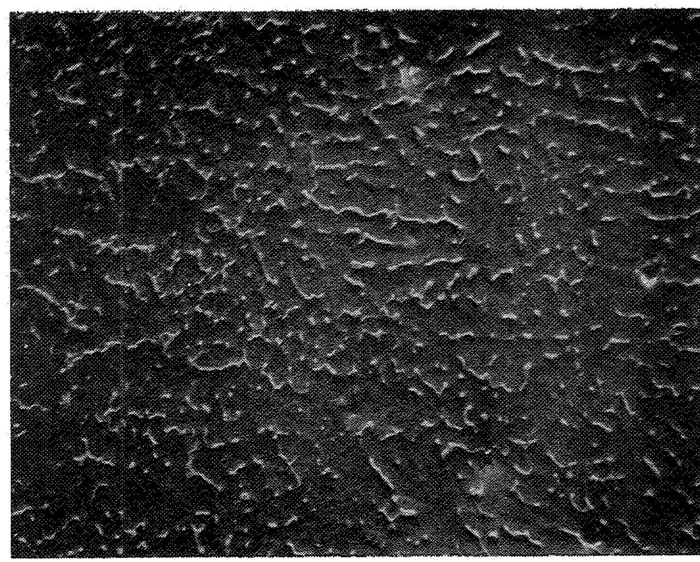

Root Region, Dendritic Structure

Fig. 2 Fusion Zone Microstructures in 2219-T87 Aluminum Ground Base Sample No. 3, 500X

B. 304L Stainless Steel

Features

1. Longer grains occur in the ground base sample rather than in the Skylab sample, maximum 0.30 mm vs. 0.14 mm.

2. Generally wider grains appear in ground base sample than Skylab sample.

3. The Skylab samples show more ordered and uniform grain growth than the ground base samples (Fig. 3).

4. Ground base samples have well-developed three-dimensional dendrites while Skylab samples have only fine cells or dendrites.

5. Entire fusion zone contains long grains in the ground base sample. In Skylab sample, only the interfacial zone has elongated grains. The thickness of this interfacial zone varies from nil to about 0.1 mm at the root.

6. Good epitaxial relation exists all around weld interface for ground base sample. Good epitaxial relations exist at bottom of Skylab sample, less perfect toward top.

7. The melt interface is much sharper in Skylab samples than in ground base samples (Fig. 3).

8. Some grains appear to have been rotated 90°, or grow perpendicular to others in the ground base sample; fewer such grains appear in Skylab sample.

9. No fine-grained, first solidification layer is present at the weld interface, both for ground base and Skylab samples.

10. The grain structure in the base metal is not appreciably affected in the nonfusion zone, except for annealing twins near the interface

11. Dendrites are thicker at the ripples in the Skylab sample No. 7.

12. The ripples are sharper in 304L stainless samples than in 2219-T87 samples.

C. Tantalum

Features

1. Grain growth morphology in tantalum samples is completely different from that in 2219-T87 aluminum and 304L stainless steel samples. Ground base grains are curvedly elongated while the Skylab sample is nearly equiaxed.

2. Ground base and Skylab samples have comparable widths of fusion and heat-affected zones.

A notable common observation (features A1, A2, B1, C1) for all three materials is that the ground base samples have longer and larger grains when compared to the Skylab samples. This major difference has, of course, been previously observed by McKannan et al. (Ref. 1). These and other features (A3, A4, B3, B4, B5) can be explained on the basis of constitutional supercooling in the manner we previously proposed (Ref. 4). Namely, the grain growth in the central or core regions of the welds must be greatly affected by gravity effects. Specifically, in the ground base samples, convection currents increased the effective liquid mixing effects, so that the solute segregation extended over much longer distances into the melt. The interfacial solute concentration and concentration gradient must be relatively small; constitutional supercooling must therefore be relatively unimportant in the ground base samples. Thus the nucleated grains in the ground base samples grew in an uninterrupted and well-oriented manner deep into the melt. In the Skylab samples, the grain or particle growth readily encountered significant constitutional supercooling as a result of the reduced effective liquid mixing, which prevented further growth and also allowed additional, and repeated, within-melt nucleation at locations ahead of the existing solid-liquid interface, resulting in fine textures.

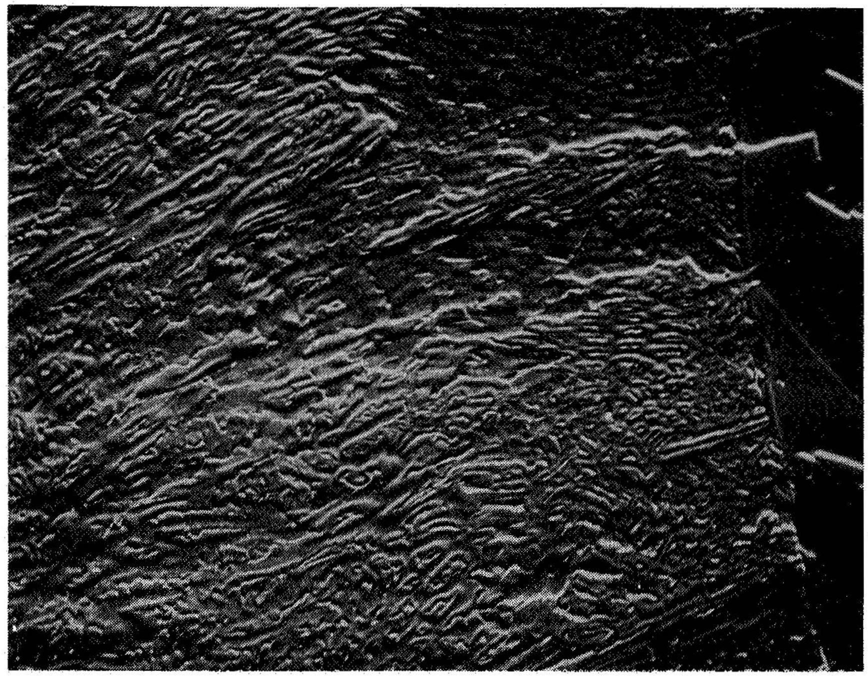

Skylab, Sharp Interface, Ordered and Uniform Growth

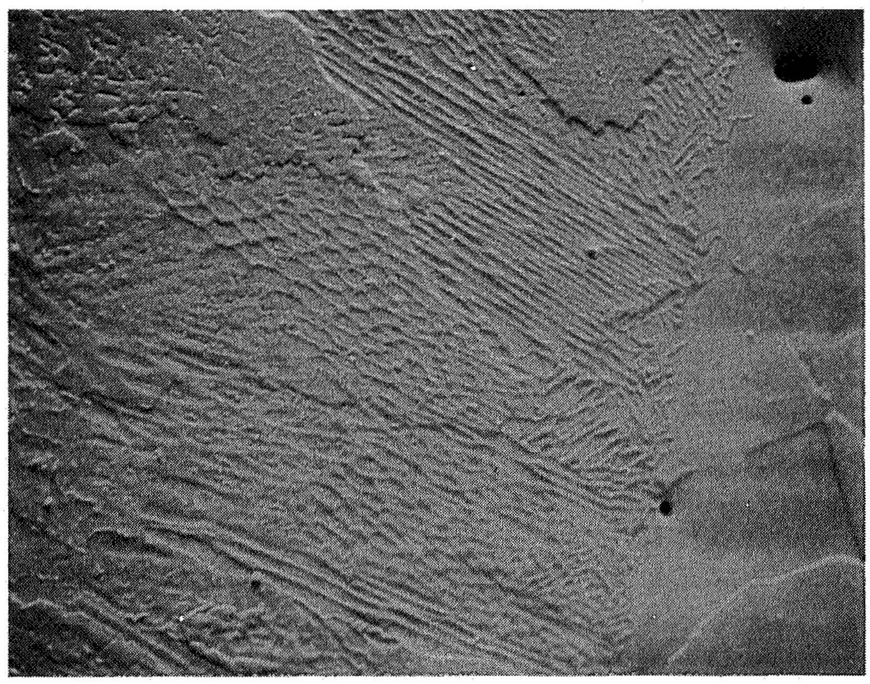

Ground Base, Less Sharp Interface, Less Ordered
and Non-Uniform Growth

Fig. 3 Interfacial Microstructures in 304L Stainless Steel Sample No. 7, 500X

We also predicted (Ref. 4) that the Skylab welds should be stronger and more uniform than ground base samples. This conclusion has been supported partly by some Russian work (Ref. 5) and partly by features A4, B3, B4, B5 and microhardness results reported later in this memorandum.

A detailed, scientific explanation of the many other relevant solidification and fluid phenomena in the welds is beyond the scope of this report. Some comments, however, follow.

None of the many above observed features can be explained on the basis of surface phenomena, including Marangoni effects (Ref. 6). Surface evaporation extends only to Angstroms or microns in depth (Refs. 7, 8). Since the melt interface is exactly at the same fixed temperature, there are no surface tension gradients along the interface. Further, microgravity should not affect evaporation, phase diagram, or surface tension.

We believe that the ripples, like all other features, are not there by chance. Rather, they exist for good reasons. In addition, we think they are very important in elucidating many of the growth features in the weld samples. According to Dr. Tobin of Westinghouse (Ref. 3), these ripples may be caused by (1) oscillatory melting and solidification, (2) liquid sloshing in the weld cavity, (3) gear noise in the drive train, and/or (4) oscillations in the power source.

We believe that the oscillatory melting and solidification mechanism arising from an unstable electron beam seems to be the most viable. This is because the ripples

- have varying radii of curvatures at the tips, some suggesting deep beam penetration, as observed elsewhere
- form semiclosed loops from left to right
- generally fall along the most probable solid-liquid interfaces
- may shift sidewise, from left to right or vice versa, suggesting "walking" of the electron beam, as commonly observed.

The repeated melting and solidification, as suggested by the ripples, introduces a repeated, "fractional solidification" phenomenon. This phenomenon, combined with the absence of convection currents, has yielded some of the unique features of the Skylab welds. Specifically, the Skylab sample welds should have much purer outer zones surrounding much more impure central zones or cores in the welds. This point, however, remains to be proven although it is suggested in Fig. 1.

The continuous grain growth in 304L stainless steel (Fig. 1) suggests strong epitaxial tendency which is not easily destroyed or even modified by repeated melting and solidification.

The probable rotation or multidirectional growth, of the grains or dendrites in the ground base 304L stainless steel sample provides evidence of convection currents in the ground base samples. Such convection currents have also been indicated in some GaAs samples (Ref. 8).

The ground base tantalum sample shows grains which are not only elongated, but curved and merging from both sides toward a last-solidifying (or low melting) central plane, as could readily be predicted from the weld heat flow pattern (Ref. 9). Such welds usually are weak, both hot and cold.

COPPER SEGREGATION

Copper segregation in aluminum sample no. 1 was studied in two ways. First, the minimum and maximum copper concentration profiles were determined from microprobe results. Second, the fractional area of eutectic phase under the microprobe beam along the weld centerlines was determined. Figure 4, for example, shows SEM pictures of the localized but detailed segregation pattern and distribution of copper-rich eutectic or other particles. From both methods it was found that Skylab sample no. 1 had more of the copper-rich eutectic phase than ground sample no. 1. Figure 5 gives the fractional areas of eutectic phase along the centerline of the welds, from the top surface down through the fusion zone into the nonfusion base metal.

Except for two readings (at locations 1 and 3) where the ground base sample had slightly more eutectic than the Skylab sample, the ground base sample was markedly poorer in eutectic than the skylab sample. The average eutectic fraction above the weld interface in the ground base sample was only 7.3 vs 12.3% for the Skylab sample, a difference significant at the 99.9% level.

The copper concentration profiles in the ground base and Skylab sample no. 1 are given in Table 1. These results show that

- the average minimum copper concentration was slightly but significantly higher (statistically 99.5%) in the Skylab sample than in the ground base sample, i.e., 3.76 ± 0.18 w/o vs. 3.34 ± 0.07 w/o
- the maximum copper concentration was markedly and significantly higher (99.9%) in the Skylab sample than in the ground base sample, i.e., 7.96 ± 0.29 vs. 5.63 ± 0.12
- the standard deviations of both maximum and minimum copper concentrations were higher (99% significant) in the Skylab sample than in the ground base sample.

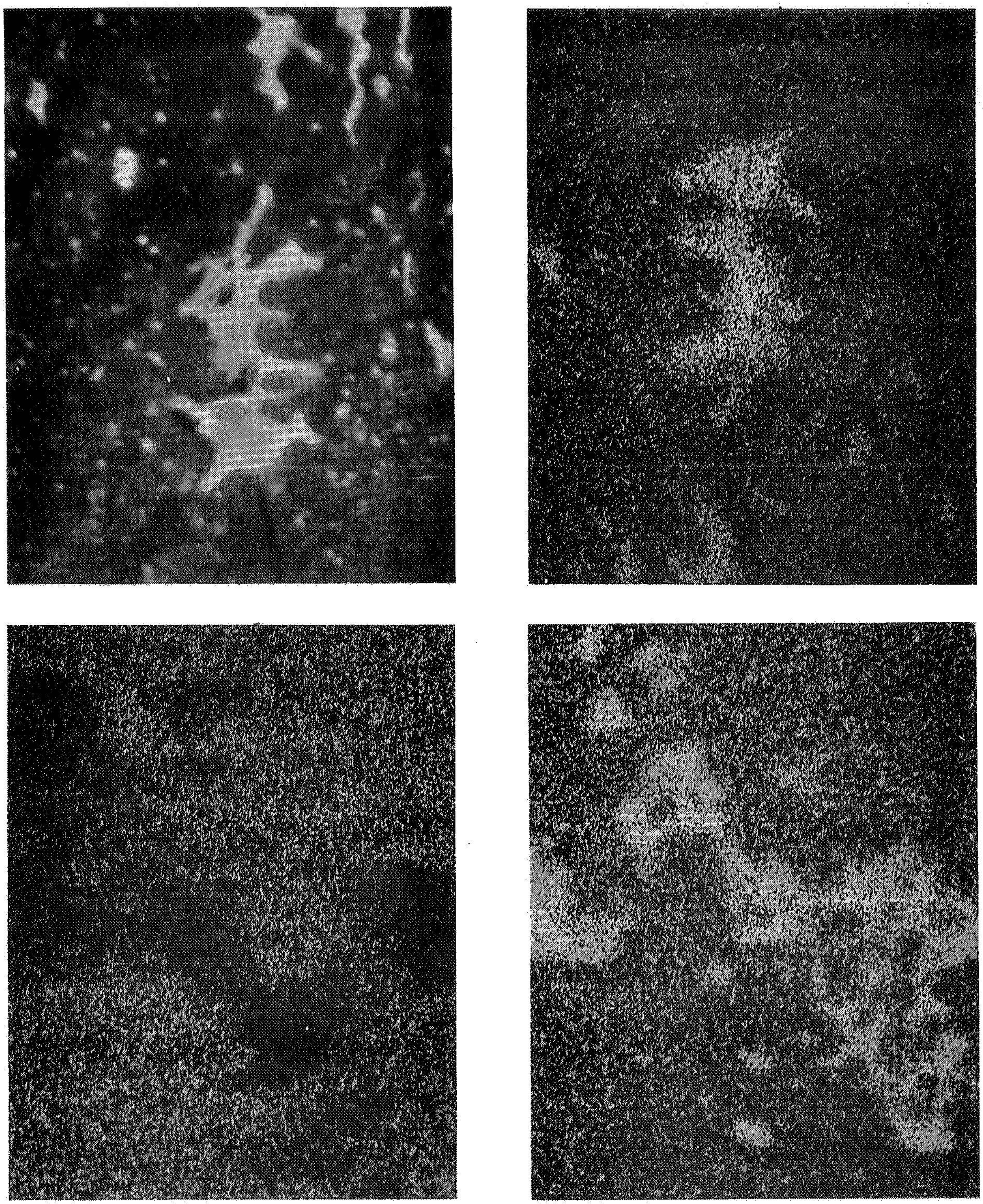

Fig. 4 Copper Segregation in Eutectic **Particles** of 2219-T87 Aluminum Skylab Sample No. 3 in Heat Affected Zone, 1350X

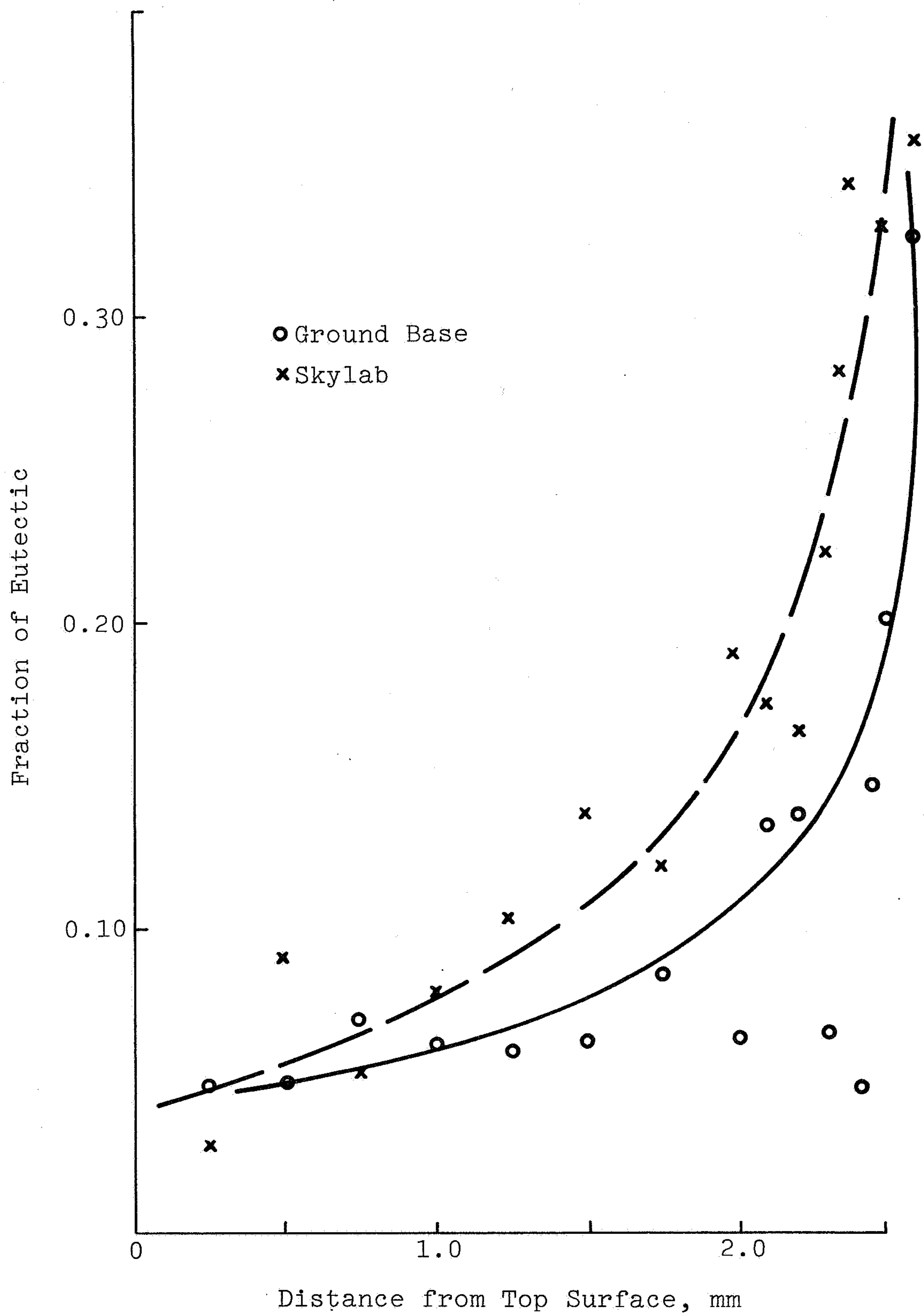

Fig. 5 Fraction of Eutectic Along Centerline of Weld in 2219-T87 Aluminum Samples No. 1

Table 1. Cu w/o in Al Sample No. 1

Distance from top surface, mm	Ground Base C_{min}	Ground Base C_{max}	Skylab C_{min}	Skylab C_{max}	
0.0	--	--	3.9	4.7	
0.25	3.4	4.8	4.0	6.6	
0.50	3.3	4.9	4.4	5.9	
0.75	3.1	5.4	4.5	6.8	
1.0	3.6	5.5	3.5	6.6	
1.25	3.4	5.0	2.9	7.1	
1.50	3.35	5.25	3.6	7.2	
1.60	--	5.8	--	--	
1.70	3.3	4.9	4.2	9.7	
1.80	3.0	7.25	--	--	
1.9	--	--	--	--	
2.0	--	--	3.1	8.3	
2.1	3.15	7.3	4.1	8.9	
2.2	3.9	5.8	3.7	10.2	Fusion Zone
2.3	3.1	4.5	3.15	13.5	INTERFACE
2.4	3.85	9.7	3.6	13.4	
2.5	3.85	13.3	4.3	14.6	Non-Fusion Zone

Fusion zone above weld interface

No.	11	11	12	12
Avg	3.34	5.63	3.76	7.96
Stand Dev	0.24	0.41	0.62	1.0
σ for Avg	0.072	0.12	0.18	0.29

The two previously described ways of studying copper segregation in the aluminum samples give practically the same conclusion, i.e., the Skylab sample had more copper segregation. The large difference in maximum copper concentration can be partly explained on the basis of constitutional supercooling while the slight difference in minimum copper concentration is mainly due to the finer grain or dendrite size in the Skylab sample as compared to the ground base sample, i.e., 10 microns vs 20 microns.

Figure 5 and Table 1 show that the copper concentration decreases from the interface toward the crown. This result, not explainable on the basis of freezing concentration (Ref. 10) according to the Al-Cu phase diagram (Ref. 11) has been qualitatively observed before (Ref. 12).

MICROHARDNESS

Microhardness transverses were made in the horizontal and vertical directions on the cross section, as well as along the weld on each set of ground base and Skylab samples, as shown in Fig. 6.

The microhardness data for each set of ground base and Skylab samples were plotted with the same centerline of weld. Examination of these plots failed to reveal any significant differences between the ground base and Skylab samples, except for the tantalum samples no. 9 (Fig. 6). A statistical summary of the data on these samples is given in Table 2.

This table shows that the microhardness readings in the nonfusion zone to the left of the fusion zone have nearly the same average value and standard deviation as those in the nonfusion zone to the right of the fusion zone. This is true for both the ground base sample and the Skylab sample no. 9. Hence, the two averages and the two standard deviations for the two nonfusion zones on each sample can be combined together for improved estimates of these two statistical parameters. Using these two combined parameters, i.e., two improved averages and two improved standard deviations for the nonfusion zones on the two samples, we can compare the nonfusion zone with the fusion zone as to

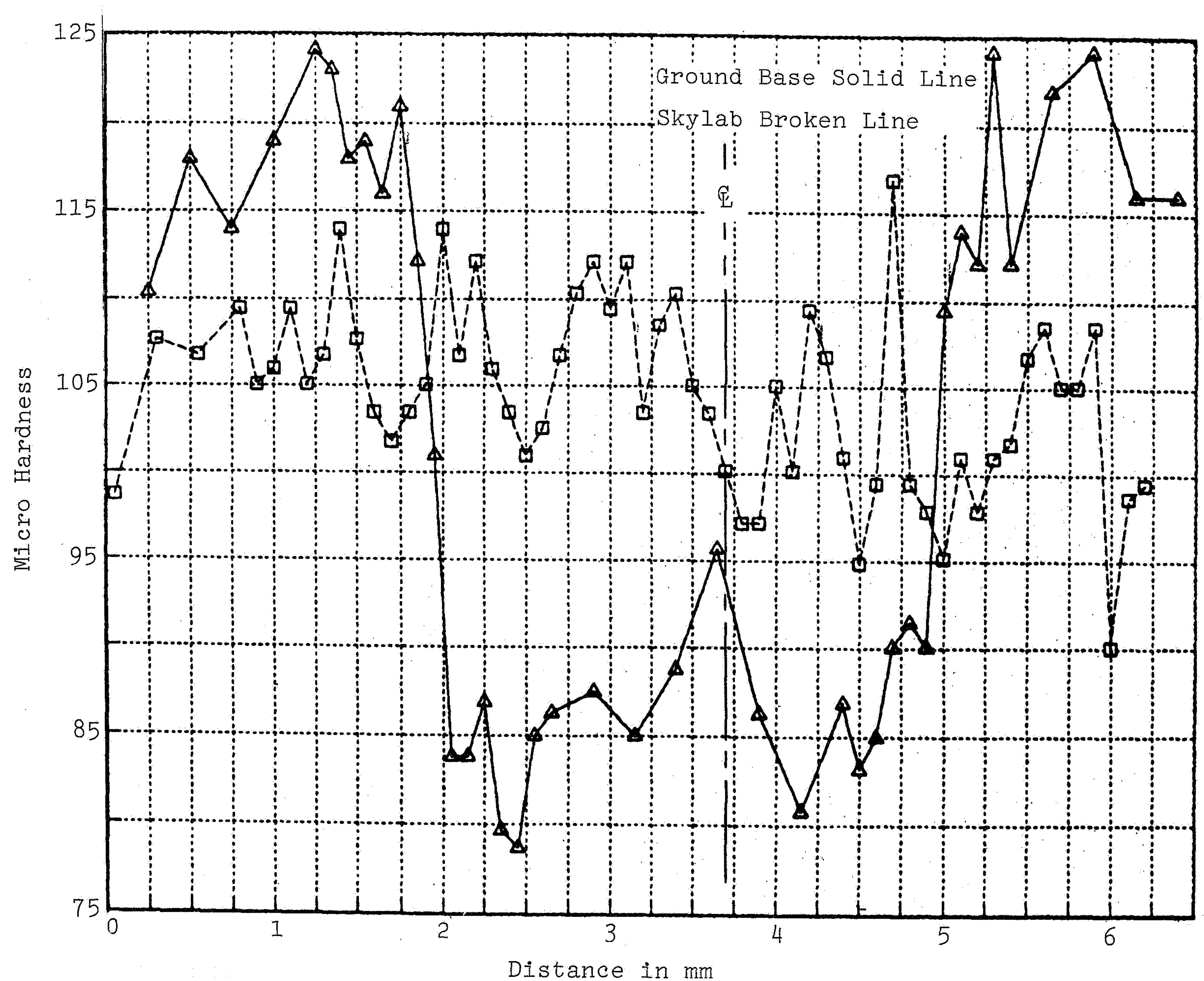

Fig. 6 Microhardness on Cross-Section Ground Base Vs. Skylab, Sample No. 9

microhardness results. Variance ratio tests (Ref. 13) show that in considering standard deviations only there is no significant (<90%) difference between the fusion zone and nonfusion zone results, both on the ground base and on the Skylab sample.

The average fusion zone microhardness is nearly the same as the average nonfusion zone microhardness (105.4 vs. 104.2) on Skylab sample no. 9. On ground base sample no. 9, however, the average fusion zone hardness is significantly (99.5%) lower than the nonfusion zone hardness.

Table 2. Summary of Microhardness on Sample No. 9

Sample	Region	Test No.	No. of Tests	Average	Standard Deviation
Ground Base	Left of fusion zone	1-11	11	117.7	3.6
	Right of fusion zone	33-41	9	116.7	4.9
	Nonfusion zone	1-41	20	117.2	4.2
	Fusion zone	12-31	20	86.8	3.2
Skylab	Left of fusion zone	1-21	21	106.4	3.6
	Right of fusion zone	41-58	18	101.6	3.8
	Nonfusion zone	1-58	39	104.2	3.7
	Fusion zone	22-40	19	105.4	4.0

This shows that, at least on the tantalum samples, Skylab welds were more uniform and probably stronger than nearly identical ground base welds, in accordance with our previous predictions. Why the other weld samples do not show this trend, or any trend at all, remains to be answered.

Variations in adjacent microhardness readings have been noted on all ground base and Skylab samples. Close examination of these variations on both samples fails to show any correlation with suspected microstructure characteristics such as grain size, aspect ratio, closeness to grain boundaries. These variations are thus likely due to experimental errors in the hardness testing. Notwithstanding such errors, the previous statistically significant conclusion as to improved strength and uniformity of weld remains valid.

SUMMARY

Results gathered by us so far further justify our use of the bulk-related, constitutional supercooling model to explain the major difference between ground base and Skylab weld samples, i.e., large elongated grains in the former vs. nearly equiaxed grains in the latter.

These results include some new comparisons in the weld microstructure between ground base and Skylab samples, and among different regions in the same sample. Some of these differences have been explained.

The analysis of ripple formation suggests that oscillatory melting and solidification arising from an unstable electron beam is the cause. Ripple formations, we believe, must be understood first because they apparently affect certain growth features in the weld samples.

By the use of two different criteria, we found evidence of pronounced copper segregation in the Skylab weld samples. In addition, on the tantalum samples studied, we showed that the Skylab weld microhardness (and hence strength) results are better than the ground base results, in line with our previous prediction.

REFERENCES

1. McKannan, E.C., "Third Space Processing Symposium, Skylab Results," NASA/MSFC M-74-5, June 1975.
2. Poorman, R. M., NASA Techn. Memo NASA TMX-64960, MSFC, Alabama, May 1975.
3. Tobin, J. M., WANL-TME-2859, Supplement to the Final Report (M551 Metals Melting) to NASA Contract NAS8-28730, June 1974.
4. Li, C. H., Monthly Progress Report No. 10 to NASA Contract NAS8-29662, May 1974.
5. Paton, B. E., et al., Automatic Welding (Russian), 5, (206), 7, 1970.
6. Bikerman, J. J., Surface Chemistry, Academic Press, New York, 1958
7. Li, C. H., "Segregation Effects During Solidification in Weightless Melts," Final Report to NASA Contract NAS8-27891, June 1973.
8. Li, C. H., "Segregation Effects During Solidification in Weightless Melts," Final Report to NASA Contract NAS8-29662, July 1975.
9. Savage, W. F., et al., Welding J., 48, 1968, p. 522-5.
10. Li, C. H., "Freezing Segregation in Alloys," Materials Science and Technology, Vol. 8, H. H. Herman, ed., Academic Press, New York, 1975, pp. 177-214.
11. Hansen, M., Constitution of Binary Alloys, 2nd Ed. McGraw-Hill, New York, 1958.
12. D'Annessa, A. T., Welding J., 45 1966, p. 579S.
13. Cramer, H., Mathematical Methods of Statistics, Princeton Univ. Press, Princeton, New Jersey, 1958.